Electronic Supplementary Information

Vertical sidewall electrodes monolithically integrated into 3D glass microfluidic chips using water-assisted femtosecond-laser fabrication for *in situ* control of electrotaxis

Jian Xu,*[a] Dong Wu,[a] Joanna Y. Ip,[b] Katsumi Midorikawa [a] and Koji Sugioka*[a]

[a] RIKEN Center for Advanced Photonics, 2-1 Hirosawa, Wako, Saitama 351-0198, Japan. E-mail: ksugioka@riken.jp, jxu@riken.jp; Fax: +81 48 462 4682; Tel: +81 48 467 9495

[b] RNA Biology Laboratory, RIKEN, 2-1 Hirosawa, Wako, Saitama 351-0198, Japan.

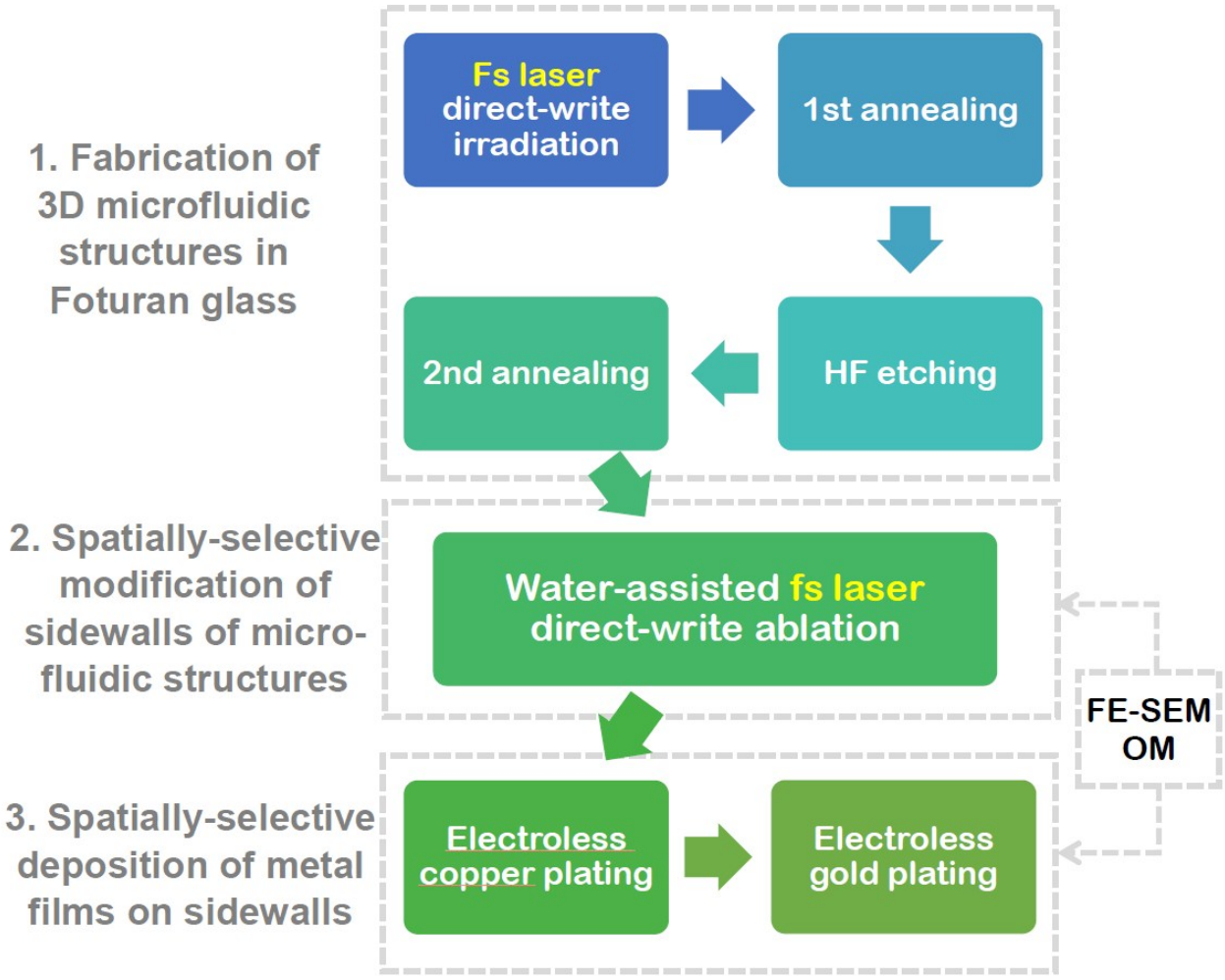

Scheme 1. Flowchart of the proposed methodology for sidewall metal patterning in glass microfluidic structures. The whole process mainly consists of three steps: fabrication of 3D glass microfluidic structures (fs laser direct-write irradiation of Foturan glass followed by annealing, HF (hydrofluoric acid) etching and additional annealing process), water-assisted fs laser direct-write ablation for spatially-selective modification of sidewalls of microfluidic structures, and electroless copper plating followed by gold plating for spatially-selective deposition of metal films on sidewalls. FE-SEM (field-emission scanning electron microscopy) and OM (optical microscopy) observation are used for evaluation of the laser-structured microfluidic structures and the plated metal films.

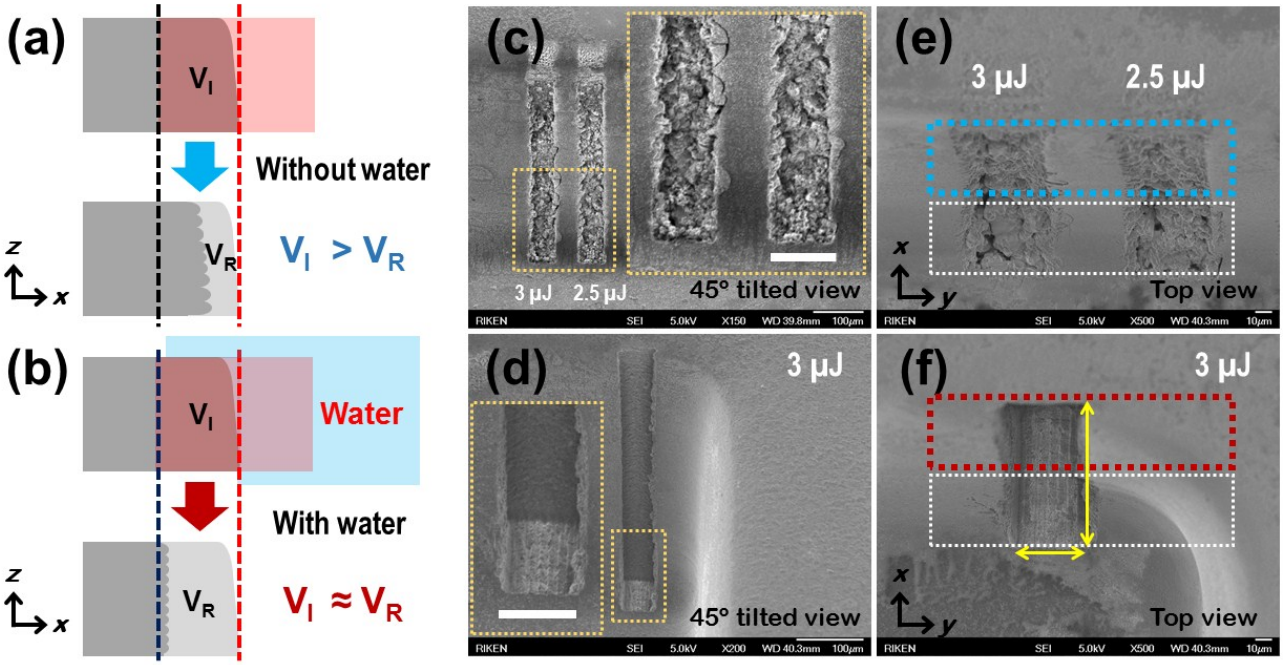

Figure S1. Comparison of the volumes removed from the sidewalls of open microreservoirs using a femtosecond-laser volume-writing scheme with and without water. (a) and (b) show the relationship between the volume of the laser-irradiated regions (V_I, the red parts) and that of the removed regions (V_R, the bright gray parts) for a pulse energy of over 2.5 µJ without and with water, respectively. The red and black dashed lines show the initial position of the sidewall and the laser volume-writing border in the glass, respectively. (c) and (d) are 45º-tilted SEM images of ablated grooves formed on the 400-µm-high sidewall surfaces of open microreservoirs using a laser volume-writing scheme without the introduction of water at pulse energies of 3 µJ and 2.5 µJ and with the introduction of water at a pulse energy of 3 µJ, respectively. The insets in (c) and (d) show magnified images (45º-tilted view) of the dashed regions; the scale bars are 50 µm. (e) and (f) are top-down SEM images of the two grooves in (c) and the single groove in (d), respectively. In these observations, the imaging plane was set at the bottom of the microreservoir so that the ablated regions at the bottom of the microreservoirs can be clearly observed. These regions are indicated by the dashed white rectangles. The ablated regions of the sidewall in (e) indicated by the dashed blue rectangle are unclear probably because the ablated volume was smaller than the writing volume ($V_I > V_R$). In contrast, the ablated region in the sidewall in (f) indicated by the dashed red rectangle is still clear, indicating that the water efficiently reduces the redeposition of debris in the interior of the glass. For this reason, the ablated volume was almost completely removed ($V_I \approx V_R$). The area indicated by the two yellow arrows is 100 × 50 µm and corresponds to the laser scanning region in the *x*-*y* plane (the irradiated volume is ~100(*x*) × 50(*y*) × 400(*z*) µm^3, the scanning length along the sidewall of the microreservoir is ~50 µm).

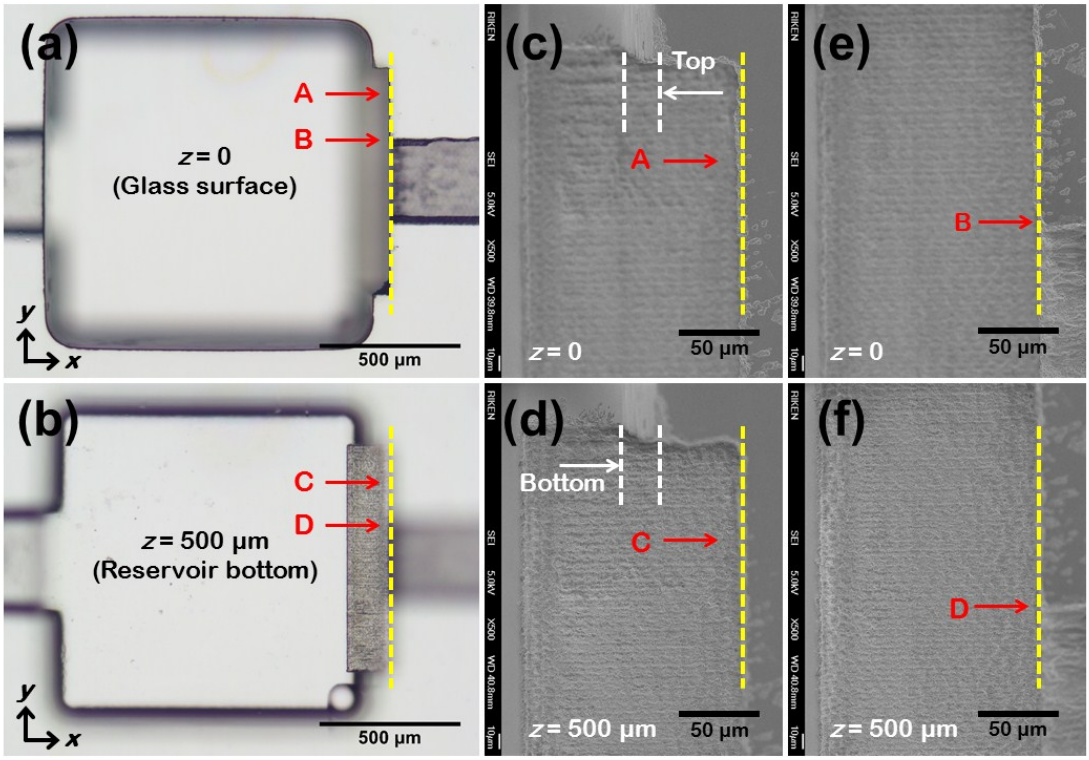

Figure S2. Efficient removal of debris using a water-assisted laser volume-writing scheme (pulse energy: ~2.5 μJ, line-by-line scan speed: 500 μm/s, line-by-line scan spacing: 3 μm, layer-by-layer scan pitch: 10 μm, scan depth in the z direction: ~330 μm, irradiation volume: ~150(x) × 800(y) × 500(z) μm^3). (a) and (b) Top-down optical microscope images of a laser-removed area in an open microreservoir. The imaging planes are at different positions on the z-axis: (a) z = 0 (glass surface); (b) z = 500 μm (reservoir bottom). (c) - (f) Top-down SEM images of a laser-removed area in an open microreservoir sidewall. Imaging plane: (c) and (e) z = 0 (glass surface); (d) and (f) z = 500 μm (reservoir bottom). The yellow dashed lines show the edge of the laser scanning area in the x-y plane, indicating that the debris generated in the glass was completely removed and the reconstructed sidewalls were nearly perpendicular to the bottom of the microreservoir when water was introduced. The arrows A, B, C and D highlight regions of interest across the images. Two white dashed lines in (c) and (d) show the horizontal distance between the top and the bottom of the sidewall, indicating the sidewall of the open microreservoir is not vertical due to different exposure times to hydrofluoric acid during the wet etching process and also different melting behaviours at the positions of sidewalls along the depth during the annealing process.

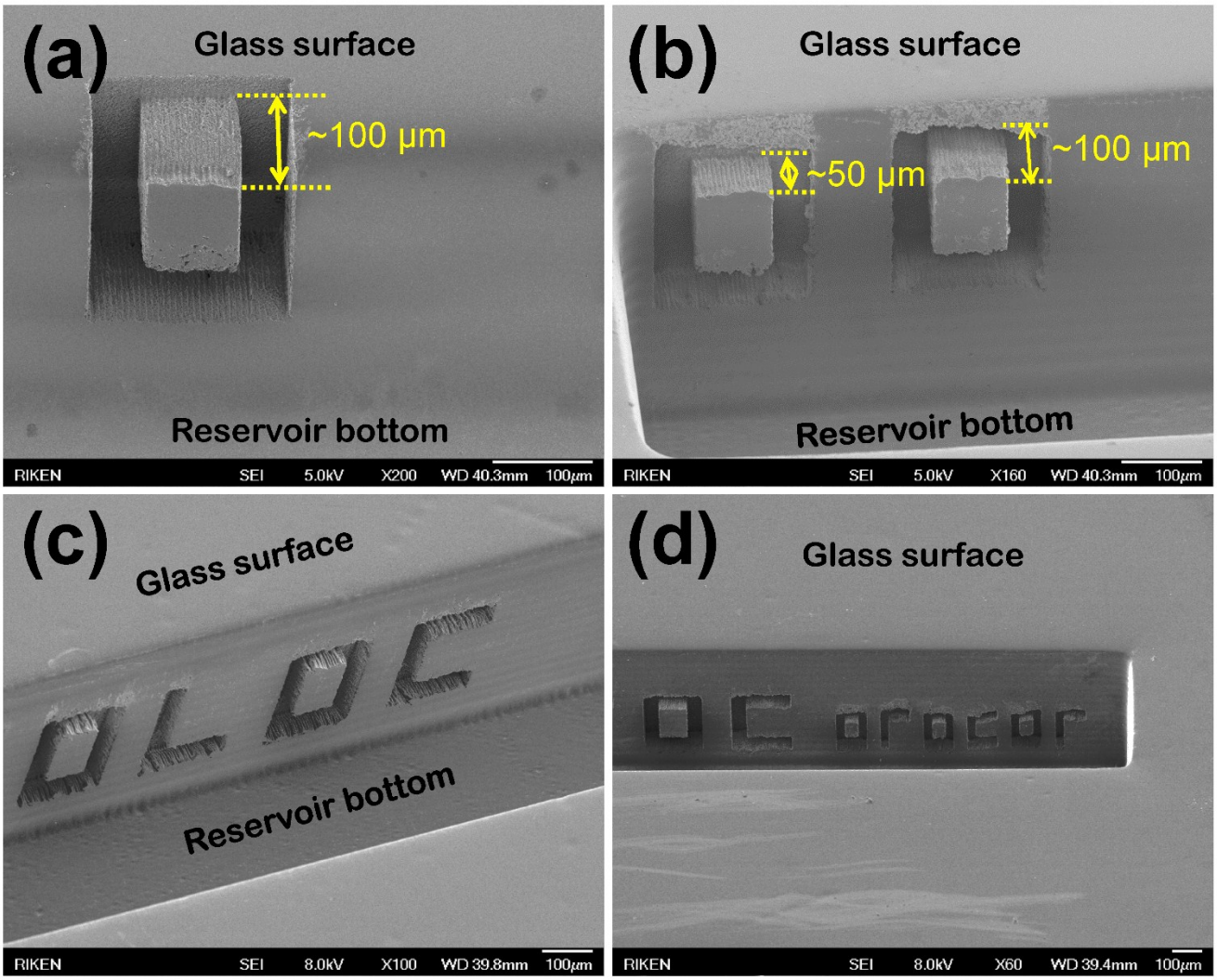

Figure S3. 45º-tilted SEM images of ablated patterns on the sidewall surfaces of open microreservoirs. (a) O-shaped pattern with a well-defined edge and a lateral etching depth of 100 µm. (b) O-shaped patterns with different lateral etching depths. (c) Micropatterns with different shapes. (d) Micropatterns with different feature sizes.

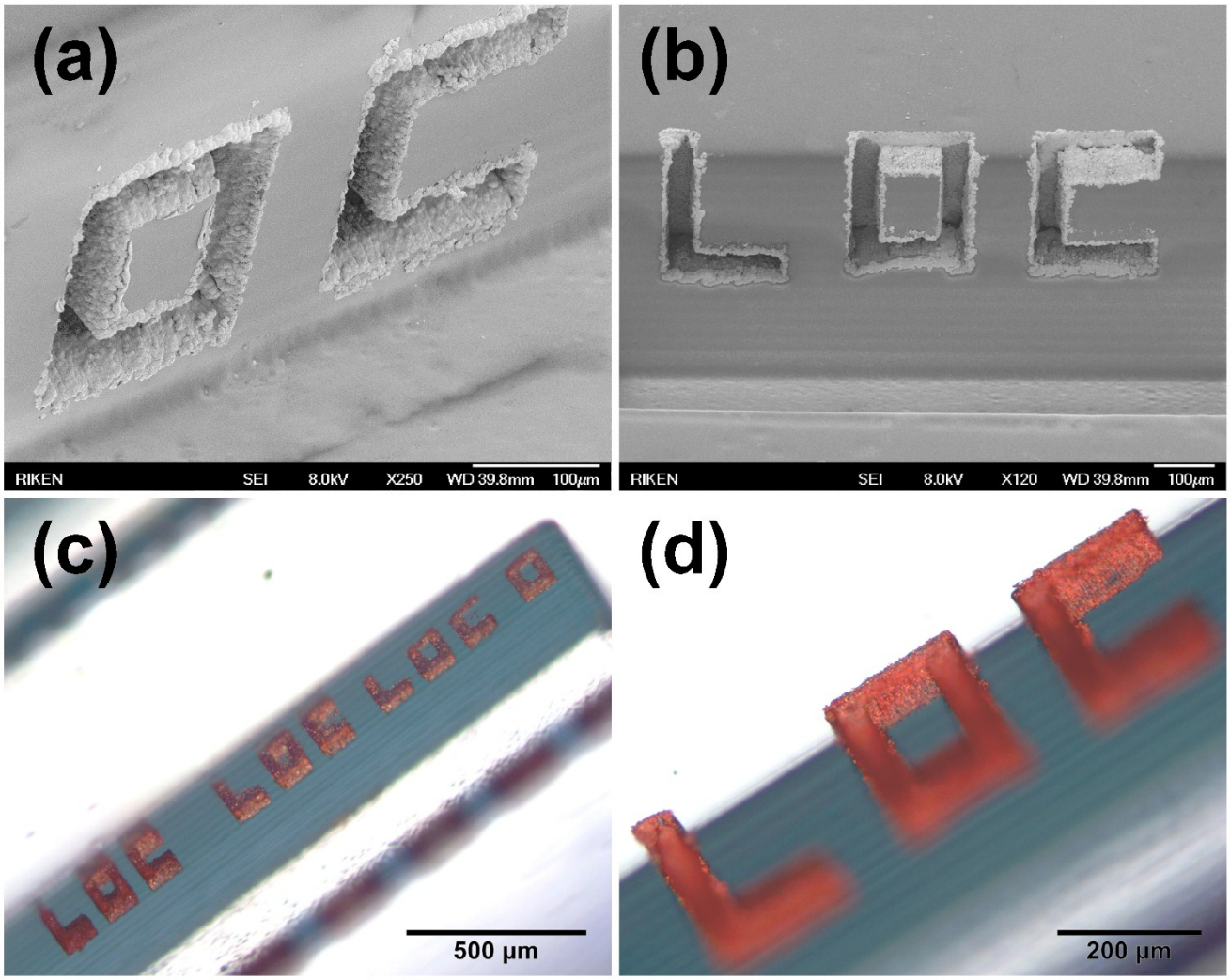

Figure S4. 45º-tilted ((a) and (b)) SEM images of metallized patterns clearly demonstrating selective metal deposition in the laser-ablated structures and ((c) and (d)) optical microscope images of metallized "LOC" patterns with different feature sizes and the "LOC" pattern shown in (b).

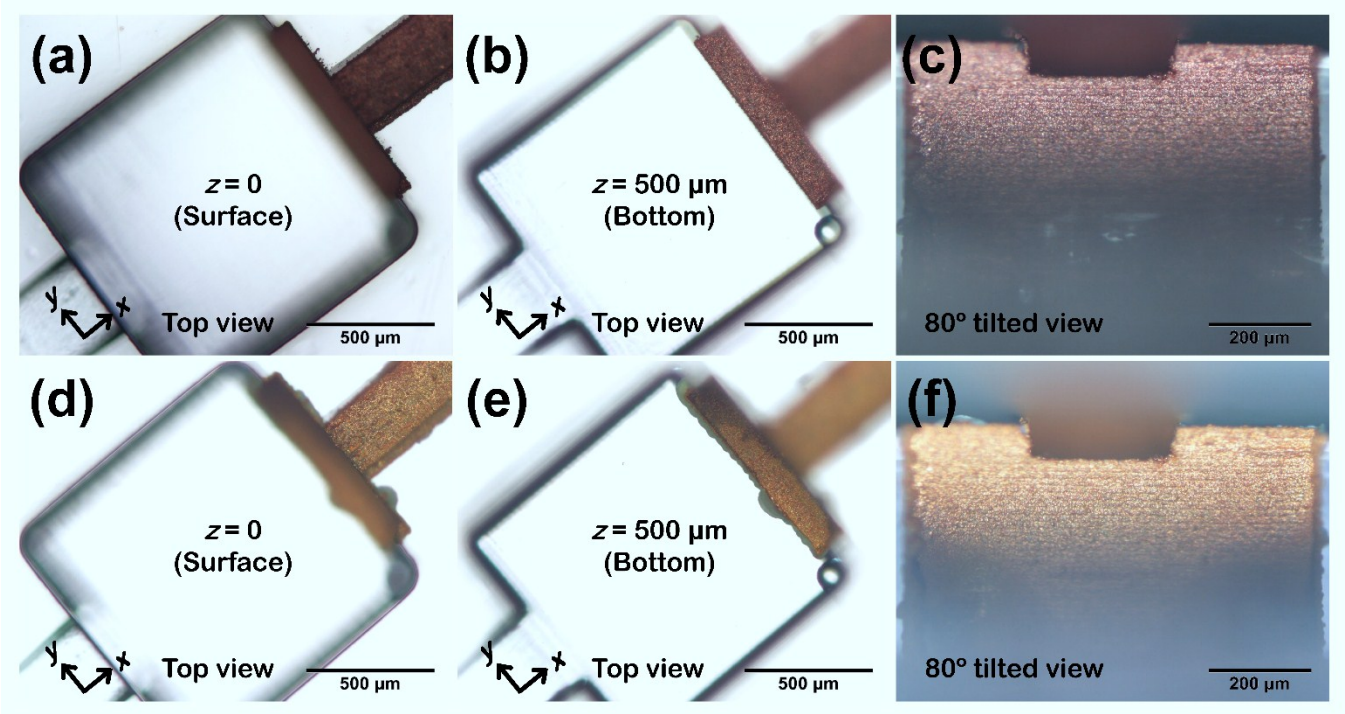

Figure S5. Top-down optical microscope images of the water-assisted laser ablated microreservoir in Fig. S2 after ((a) and (b)) electroless copper plating (~12 h) and ((d) and (e)) additional electroless gold plating (~6 h). Imaging plane: (a) and (d) glass surface; (b) and (e) reservoir bottom. Optical microscope images of vertical metal pad formed on the sidewall of the microreservoir in Fig. S2 after (c) electroless copper plating and (f) additional electroless gold plating. To obtain (c) and (f), the samples were tilted by ~80º with respect to the direction of observation. The recessed structures observed on the top of the sidewalls in (c) and (f) were created by laser ablation to produce metal interconnections on the glass surface. The height of all sidewalls shown is ~500 µm.